ACS SENSORS

pubs.acs.org/acssensors

Article

How to Identify the "LIVE/DEAD" States of Microbes Related to Biosensing

Ling Liu,* Changyu Liu, He Zhang, Jingting He, Junfeng Zhai, Dengbin Yu, and Shaojun Dong*

Cite This: *ACS Sens.* 2020, 5, 258−264

Read Online

ACCESS | Metrics & More | Article Recommendations | Supporting Information

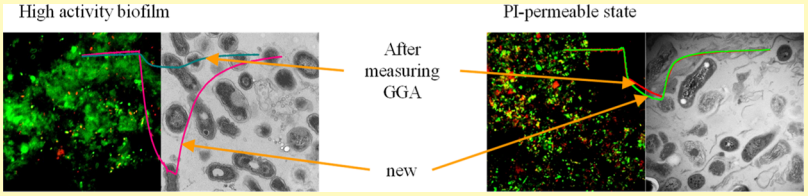

ABSTRACT: In this work, we fabricated a microbial biosensor with long-term stability, which relied on microbial activity. Activity of the microbe was commonly estimated by LIVE/DEAD assay and the propidium iodide (PI)-stained one was judged as dead. Herein, we proposed the utilization of a physiological state of microbes, which was neither live nor dead but between them. In this state, microbes represented a high PI-stained ratio but still had catalytic ability. This microbial state was obtained by forming the biofilm under the conditions of poor nutrition and low temperature. Thus, the dividing and proliferating ability of the microbes in the biofilm was weak, which was beneficial for long-term stability. This mechanism was further confirmed by the biosensors made from multifarious substrate materials, including graphene-based gel, biomass-based gel, graphite felt, and poly(vinyl chloride). This biosensor was applied to water pollution monitoring in the laboratory for 2 years and then was integrated into a multiparameter water quality monitoring station on a local lake for 2.5 years.

KEYWORDS: *biosensor, biofilm, LIVE/DEAD assay, long-term stability, water pollution monitoring*

A microbial sensor is a most commonly used tool in the water environment monitoring field. Based on the multiple intracellular enzyme systems in a microbial cell, the biosensor provides inherent benefits in multitasking for catalyzing the complex samples in the environment (e.g., for degrading the mixture composed of multiple organic compounds).[1−4] However, for fabricating a biosensor, the microbes are usually needed to be immobilized, which will expose the cells to an unnatural environment. Thus, the activity of immobilized cells will be changed[5−8] and the biosensor's performance will be affected. Therefore, the investigation on long-term stability of immobilized microbes is of great importance for the biosensors.

To detect and characterize the activity of the microbes, LIVE/DEAD kits are widely employed.[9−12] These dye kits are typically composed of two fluorescent dyes, one labels the living microbes (or all) and another for the dead. Among them, propidium iodide (PI) is a frequently used dye for the dead, such as SYTO9/PI, fluorescein isothiocyanate (FITC or marked FITC)/PI, and so forth.[13−18] The permeability difference of PI to penetrate healthy and damaged membranes is the key point for the PI staining assay. Therefore, PI is considered as a most reliable indicator for the dead microbes being an end stage of plasma membrane permeabilization.[19] Therefore, in almost all of the reports about LIVE/DEAD assay, the microbes stained with PI are judged as dead and discarded for the biosensor application. However, in this state, some microbes still have catalytic ability because their intracellular enzymes are conserved by the compromised plasma membrane. In addition, some reports indicate that except alive or dead states, the microbes also exist in various intermediate states, such as viable but nonculturable,[20,21] metabolic activity with intact energized membranes but not able to replicate, nonactive and dormant that can be injured with permeable membranes, or damaged and respiration is no longer possible.[22] Hence, the microbes stained with PI still have the potential ability to be retrieved and reproduced at some suitable conditions. Therefore, it is too rash to call the PI dyeable microbes as "dead". Some reports rationally characterized PI as the membrane intercalator,[23−25] just used to prove the membrane integrity,[26,27] or emphasized that PI-stained microbes were not lysed.[28] Thus, it raises a probability that some microbes have the compromised membranes and can be stained with PI in LIVE/DEAD assay, but they still have an applicable value in practice.

In this work, a significant relationship between the PI-stained ratio and catalytic activity of immobilized microbes was

Received: October 31, 2019
Accepted: December 26, 2019
Published: December 26, 2019

https://dx.doi.org/10.1021/acssensors.9b02138
ACS Sens. 2020, 5, 258−264

found. The immobilized microbes could actually be in a state that was PI-permeable but with long-term catalytic activity. This characteristic was beneficial for fabricating the biosensor. Therefore, a water quality monitoring biosensor with a satisfactory long-term stability was fabricated.

EXPERIMENTAL METHODS

CLSM, AFM, and TEM. Confocal laser scanning microscopy (CLSM, Nikon, C2, Japan) was used to image the spatial morphology and structure of microbes. The LIVE/DEAD assay was carried out by using FITC (Sigma) to label all microbes and PI (Sigma) to label the damaged. FITC and PI were dissolved together in phosphate-buffered saline (PBS: 0.12 M Na_2HPO_4 and 0.08 M KH_2PO_4, pH 7.0) with a final concentration of 1 and 0.05 mg mL^{-1}, respectively. The samples were incubated in the abovementioned solution for 15 min at room temperature. Before the imaging test, the samples were washed thoroughly with PBS. The excitation wavelengths were 488 and 561 nm for FITC and PI, respectively. In each imaging test, the fresh cultured microbes and the treated at 100 °C for 1 min were used as the blank and fully stained control, respectively, to ensure that each test condition was reasonable.

Intracellular structures and their changes in microbes were investigated by transmission electron microscopy (TEM) and atomic force microscopy (AFM). For TEM imaging, the ultrathin sections of microbial cells were prepared. For ultrastructural observations, biofilm samples were first fixed using 2.5% glutaraldehyde for 12 h and then 1% osmium tetroxide for 2 h at room temperature, then dehydrated with a graded ethanol series (50, 70 and 90%) for 15 min each, and then dehydrated with 100% ethanol 3 times and 10 min each time. Samples were embedded into the Eponate 812 resin and polymerized for 8 h to obtain solid blocks. Ultrathin sections (50−70 nm) of the sample blocks were cut by using a Leica UC6 microtome (Leica, Vienna, Austria) with a diamond knife (Diatome, Switzerland). TEM images were obtained by using H-7650 TEM (Hitachi, Ibaraki, Japan) at 80 kV of accelerating voltage. Damages of microbial cells were characterized by using an AFM MultiMode 8-HR microscope (Bruker) with the probe model: SCANASYST-FLUID+.

Biosensor. A biosensor with the biofilm as the signal generator was fabricated based on a flow system. An electrochemical workstation (CHI 832, CHI Co., Shanghai, China) was used as the signal collector. A constant temperature incubator was used to maintain the temperature of the biosensor. Peristaltic pumps (Longer BT100-1J, Baoding, China) and several solenoid valves were used to drive the flow system. A fixed flow rate of 2.5 mL min^{-1} was set for all of the experiments. The sensor was maintained by circulating PBS when it was not in use. The organic substances were obtained by diluting the GGA1980 solution that composed of 1.5 g L^{-1} glucose and 1.5 g L^{-1} glutamic acid (analytical reagent grade, Beijing, China).

Biofilm and Suspended Microbes. The biofilm was cultured by using the present flow system on a graphene-based gel, Gel_{rGONR}, reported by our previous work.[29] The Gel_{rGONR} was put in a columned chamber made of polymethyl methacrylate with 2 cm depth and 1 cm diameter for a total working volume of 1.57 mL. First, the entire system was sterilized with 75% alcohol and washed with PBS, and then, an inoculated nutrient solution prepared by adding one-tenth of LB medium (tryptone 10 g, NaCl 10 g, and yeast extract 5 g in 1 L medium, pH 7.0) into PBS was pumped continuously through substrates of biofilms under 35 °C. After 12 h, the PBS solution was pumped to remove the redundant medium. The temperature in the chamber of the biosensor was set at 30 °C for maintaining the stability of microbial activity of the biofilm. The substrates of biofilms can be replaced by graphite felt, biomass-based gel, poly(vinyl chloride) (PVC), and other materials. As shown in Scheme S1a, for biofilm experiments, the inoculated nutrient solution, PBS, organic substances, and toxic substances were pumped into the biosensor via the flow system. For morphological characterization, the biofilm was carefully scraped from the substrate or inner surface of tubes by using a sterile pair of tweezers. For the suspended assay (Scheme S1b), the microbes were cultured in a flask by using a constant temperature oscillation incubator under 37 °C, 220 rpm. After 12 h of incubation, the bacterial suspensions were collected by centrifuging at 4000 rpm for 3 min and resuspended in PBS and then treated by adding toxicants to obtain the PI-permeable state.

Electrochemical Measurement. As shown in Scheme S1, two states of microbes, the suspended and the biofilm, were compared in the present work. All of the electrochemical signals were obtained by using two CHI 832 electrochemical workstations. The setup of the electrochemical workstation was conducted by applying a constant potential of −700 mV versus Ag/AgCl (0.1 M KCl), which is the potential for detecting dissolved oxygen (DO). For the suspended microbes, chronoamperometry was performed by using a Au array working electrode (φ = 50 μm × 20) with one piece of Pt as counter electrode for recording catalytic signals. For the biofilm in the biosensor, the $I-t$ curve mode was adopted. A three-electrode DO probe, with a Au working electrode (φ = 0.8 mm), an assembled Pt wire as the account electrode, and the Ag/AgCl reference electrode, covered by a Teflon membrane (Orbisphere 2956A) was used for all current signal measurements.

Colony Forming Units. About 1 mm^3 bulk of the biofilm was picked up by using a sterile pair of tweezers and transferred into 2 mL of sterilized PBS. The same biomass of fresh microbes was controlled by using a UV−vis spectrophotometer (INESA) according to the optical density at 600 nm (OD_{600}). These dilutions were cultivated by the spread on LB culture medium (by adding 2% agar), and colony forming units (CFU) were counted. A blank was made by adding sterilized PBS instead of the sample.

RESULTS AND DISCUSSION

Typical LIVE/DEAD Assay and PI-Permeable State. The fresh microbes, cultured by using a flask in a shaking incubator, were employed as the control test. As shown in Figure 1a, the 9% PI-stained rate was obtained by CLSM images and the intact cellular morphology was shown by TEM images. An obviously catalytic signal for catalyzing GGA20 by these microbes is shown in Figure 1e (black curve). The same microbes were treated by the thermal method at 100 °C for 1 min, from the CLSM images in Figure 1b, and a nearly one hundred percent PI-stained ratio was obtained. Its corresponding electrochemical signals exhibited that the catalytic activity of these microbes was almost depleted (the red curve in Figure 1e). This result indicated that microbes stained with PI were dead or at least lost their activity, which was a general result by LIVE/DEAD assay.

When microbes were immobilized by forming a biofilm, the PI-stained ratios were close to one hundred percent for both the fresh (Figure 1c) and the used biofilm by measuring glucose and glutamic acid (GGA) for 2 months (Figure 1d). In TEM images, the intracellular structures of these microbes were changed seriously and some microbial cells even began to exhibit a closed lysis state. Judging by the traditional definition, the present results suggest that all of the microbes in the present biofilm were "dead" or "near-dead". However, in Figure 1f, the uniform electrochemical catalytic signals toward GGA20 were obtained by these two biofilms (curves a and c). This was an interesting phenomenon that the microbial cells in the biofilm were "dead" judging by the LIVE/DEAD assay, but they still had the normal catalytic activity toward GGA20, and this state could be maintained for a very long term. The results indicated that the intracellular catalytic system, mainly including the enzymes and so forth, was maintained well by the present biofilm formation.

Conditions for Obtaining the PI-Permeable State. It was noticed that the PI-permeable state microbes maintained their activity by forming the biofilm but not by the suspended,

https://dx.doi.org/10.1021/acssensors.9b02138
ACS Sens. 2020, 5, 258−264

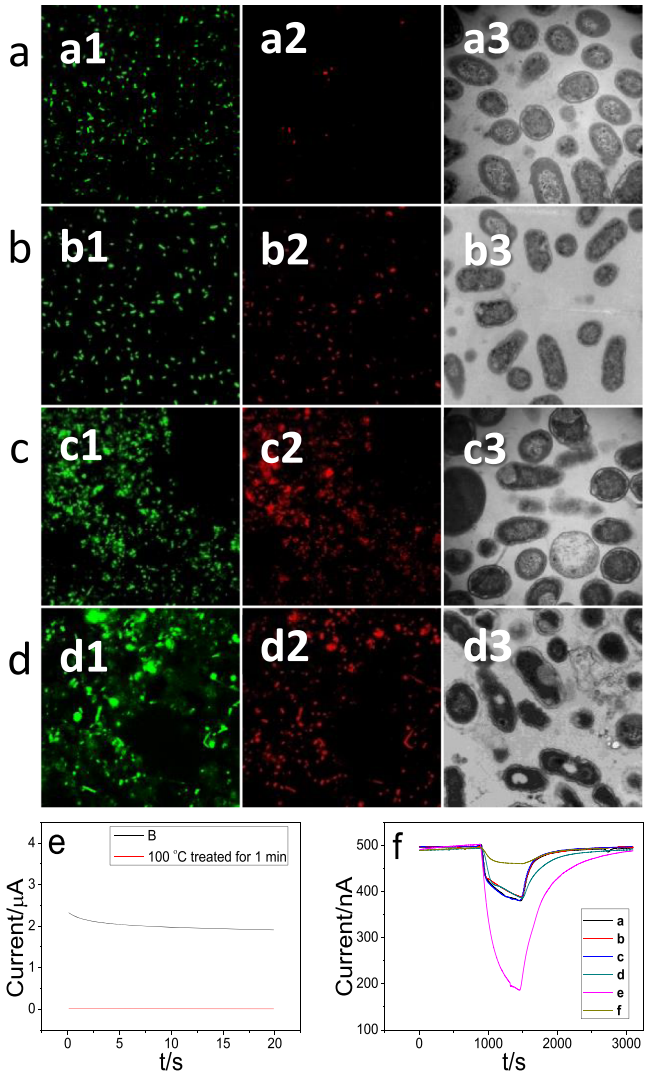

Figure 1. Fresh microbes (a) and those treated by the thermal method at 100 °C for 1 min (b), new cultured biofilm (c), and used to measure GGA for 2 months (d). From (a–d), (1) FITC-stained and (2) PI-stained in CLSM images and (3) TEM images. Electrochemical signals for suspended microbes (e) and for the biofilm (f). In (f), curve a was obtained with the new biofilm; curve b was obtained from a after measuring the real sample; curve c was obtained from a after measuring GGA; curve d was obtained from a after measuring the toxicant; curve e was obtained with a high-activity biofilm; and curve f was obtained from e after measuring GGA.

and a new experiment for comparing the microbes in the suspended state and biofilm in detail was carried out by testing the effect of the toxicant toward microbial activity. Based on our previous experiments, Cu^{2+} ions were chosen as the model toxicant.[30] The statistical results showed (Figure 2) that the stained rates of PI for the two assays were the same, approaching one hundred percent, which reveals that these two types of microbes were "dead" after treated with heavy metal ions (2–10 mg L^{-1} of Cu^{2+} ions in Figure S1). It was interesting that a completely opposite trend for these two microbes was obtained by the electrochemical results (black inverted triangles and black dots in Figure 2). In the suspended assay, the inhibition ratio of respiration was enhanced by increasing the concentration of Cu^{2+}, indicating that the catalytic activity of the microbes was inhibited. In contrast, in

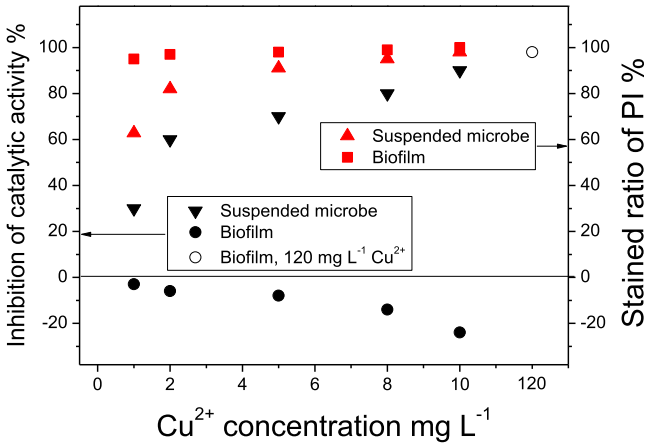

Figure 2. Comparison of the suspended microbes (red triangles and black inverted triangles) and biofilm (red diamonds and black dots) as test samples. The black circle indicates the respiratory inhibition of the biofilm by adding 120 mg L^{-1} Cu^{2+} ions.

the biofilm assay, the respiration of microbes was promoted and its degree was enhanced by increasing the concentration of Cu^{2+} ions. There were two probable reasons: one was that the toxic substance may act as the respiratory substrate and another one was that it induced a stress response of microbes.

When 120 mg L^{-1} Cu^{2+} ions were added into the biofilm system (black circle in Figure 2), a 98% inhibition was obtained by the electrochemical result. This result indicated that the Cu^{2+} ions in fact played a toxic act on the biofilm but not as the respiratory substance. Under the same Cu^{2+} concentration range, the catalytic activity of the PI-permeable microbes was related to their environment. For the biofilm, the matrix of the extracellular polymer bound the microbes into a whole and adhered to the surface of a substrate, which resulted in the microbes in the biofilm being less susceptible to toxicity. Here, a subinhibitory concentration (sub-IC) of toxic substances was employed to explain the present phenomenon.[31] Under sub-IC, the toxic substance acts as an agonist for the microbe metabolism, which induced the self-repair of microbes and thus saving it alive. Under the specific environment and sub-IC, the toxic substance would not kill the microbes, which provided a certain capacity for the self-regulation of the biofilm. This trait induced a long-term metabolic ability.

Furthermore, the other types of suspended microbes were investigated, including new cultured microbes placed in PBS for 24 h at room temperature (Figure 3a), treated with 5 mg L^{-1} Cr(VI) for 30 min (Figure 3b), killed by thermal treatment at 70 °C for 15 min (Figure 3c), and 3c was placed in PBS for 1 h (Figure 3d). PI-stained rates were 90, 98, 90, and ~100%, respectively. The electrochemical signals (3a,b) were significantly reduced compared with that of the fresh microbes (Figure 3e), indicating that the PI-permeable microbes had no catalytic activity when they were in the suspended state. There was an exceptional result with 90% catalytic activity (Figure 3c, 70 °C for 15 min). The reason may be that the microbial cells were not destroyed in such a short time. However, this state did not hold. When this microbe was placed in PBS for 1 h (curve d in Figure 3e), the activity lost, indicating that it was not a stable PI-permeable state of microbes.

The process of biofilm formation was also investigated. As shown in Figure S2, a notable increase of the biofilm mass in

https://dx.doi.org/10.1021/acssensors.9b02138
ACS Sens. 2020, 5, 258–264

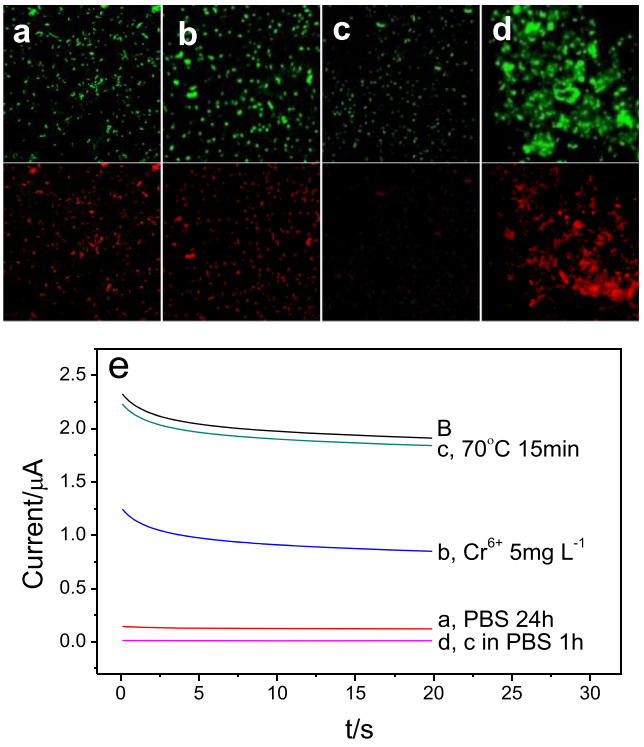

Figure 3. New cultured microbes placed in PBS at room temperature for 24 h (a), treated with 5 mg L^{-1} Cr(VI) for 30 min (b), treated at 70 °C for 15 min (c) and (c) placed in PBS for 1 h (d), and the corresponding electrochemical signals (e).

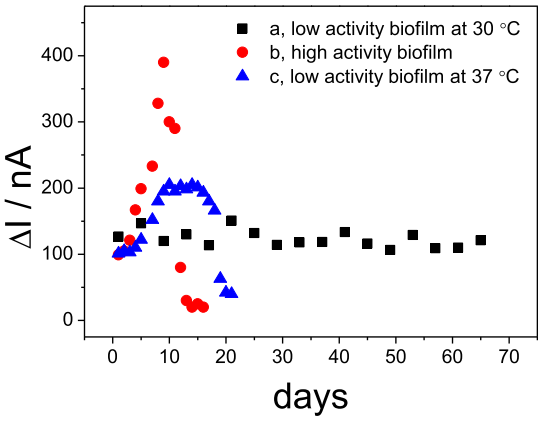

Figure 4. Electrochemical results for catalyzing GGA20 by the nutrition-poor biofilm (a, black diamonds) and nutrition-enrichment biofilm (red dots) (a) at higher temperature. The net current was obtained by subtracting the electrochemical signal of the blank (PBS) from that of the total signal (PBS and GGA20).

the lawn plate was observed within 48 h by continually pumping inoculated solution into the flow system. If judged by the LIVE/DEAD assay, the present biofilm was formed and developed by a huge mass of "dead microbes" because most of the microbes in the biofilm were stained with PI. In fact, this biofilm could give an obvious catalytic signal toward GGA (curve a in Figure 1f). By comparison, a nutrition-enrichment biofilm with high activity was also cultured, as shown in Figure S3. This biofilm could be stained with PI slightly as shown in Figure S4a and had very high activity for catalyzing GGA (curve e in Figure 1f), which was about 3 times of that obtained by the nutrition-poor biofilm initially (curve a in Figure 1f). However, this catalytic signal was reduced quickly within 2 weeks (curve f in Figure 1f), and the biomass of the biofilm was also lost because of the over-vigorous growth, so it was not stable for the biofilm compared with the nutrition-poor state (Figure S3b).

The effects of the measurement frequency and temperature were studied. The increase of the measurement frequency resulted in the catalytic activity rapidly increase and then declined sharply (red dots in Figure 4). In fact, the increase of the measurement frequency suggested the increase of the nutrition. A similar trend was obtained at a higher temperature in the columned chamber of the biosensor (blue triangle in Figure 4). Thus, a long-term application of the biofilm for environmental monitoring should be guaranteed by the conditions with poor nutrition and low temperature.

Characterizations of the PI-Permeable State. Herein, a feature was noticed that some green flocs were showed by the FITC-stained images for all of the biofilms. These flocs were the extracellular matrix composed of some exopolysaccharides, extracellular DNA (eDNA), flagellum, fimbriae, pili, and so forth. The matrix materials promoted attachment of microbes on surfaces of substrates or played a role in recruiting planktonic microbes into the biofilm.[32] These matrix networks provided a favorable ecological niche for the intracellular enzymes. Therefore, the extracellular matrix was useful for maintaining the catalytic ability of PI-permeable state microbes in the biofilm. Some components of the extracellular polymeric substance (EPS) had magical effects on living organisms, such as to form a unique protective film on the surface of the microbes under some harsh conditions such as the high temperature, high cold, high osmotic pressure, and dehydration conditions, and thus, the protein molecules were effectively protected to avoid losing their activity. Beyond that, the EPS also had the ability for extracellular electron transfer reported by Zhao et al.,[33,34] which was related with the stable electrochemical signals of the PI-permeable state biofilm.

The biosensor was applied to measure real samples, and the effects of exogenous microbes to the biofilm were investigated. As shown in Figure S5, with the change of test conditions, the microbial flora structure was changed, indicating that the biofilm could be influenced and complemented by exogenous microbes in the applied process. However, its catalytic signal remained stable (Figure 1f, curve b). This result indicated that the catalytic signals of GGA by exogenous microbes were offset under the nutrition-poor test conditions.

The AFM technique was adopted to investigate the integrity of the PI-permeable membrane of microbes. As shown in Figure 5, the microbial membrane was really incomplete (Figure 5a,b), and the microbial cells scraped from the present biofilm could not be uniformly suspended in PBS solution (inset in b), indicating that the cellular accessory constructions, such as flagella and capsular, were really damaged. To clarify the reparability of the PI-permeable membrane of the damaged microbes, a common criterion experimental CFU for detecting viable microbes was adopted. As shown in Figure 5c, after incubating under 37 °C for 12 h, microbes inoculated from the biofilm on the nutrient plat had partly regrown, which demonstrated that the microbes in the present biofilm possessed the ability to reproduce under a suitable condition. However, for the same inoculated mass, the abundance of viable cells of the biofilm was significantly less than that by fresh microbes (Figure 5d). Therefore, in the PI-permeable

https://dx.doi.org/10.1021/acssensors.9b02138
ACS Sens. 2020, 5, 258−264

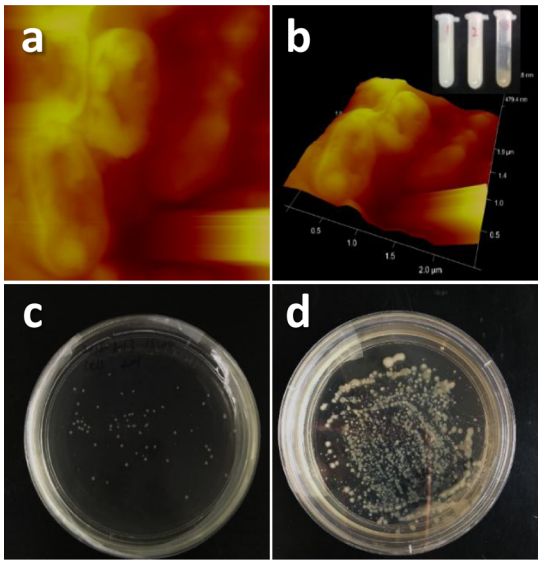

Figure 5. (a,b) AFM images for the microbes scraped off from the PI-permeable state biofilm. The inset of (b), from the left to the right, the photographs of fresh microbes, and after 1 h of incubation with the toxicant and the microbes scraped off from biofilm. cfu of PI-permeable microbes (c) and fresh microbes (d) with the same inoculated mass.

state, microbes had very weak ability to divide and proliferate. Thus, they maintained their catalytic activity for a long time at a stable level. A similar result was reported by Jimenez and Rühl et al.[35,36]

Applications of the PI-Permeable State of Microbes. Herein, a water pollution monitoring biosensor was established for detecting the biochemical oxygen demand (BOD) and water total toxicity of the water samples from a local lake. The performance of this biosensor is shown in Figure S6. A calibration curve was obtained by measuring the concentration gradient of GGA solution (Figure S6a). Based on this, by using the linear regression method, the related values of real samples were calculated by this calibration curve. In addition, the results were capable to compare with conventional BOD_5 values (Figure S6b). Furthermore, the long-term stability was estimated by measuring GGA for 2 years (Figure S7). This result indicated that the PI-permeable biofilm was really beneficial for long-term application of environmental measuring.

Here, an interesting phenomenon was noticed that the same trend for separately measuring GGA and toxicant Cu^{2+} was exhibited (Figure S8) in the measurement of the toxic substances in water by using the present biosensor. It was interesting for the condition of adding toxic substance as there were no organic substrates added, but the electrochemical signal was also reduced, indicating that the DO was reduced because it accepts the electrons transferred via the microbial respiratory chain. According to the results shown in Figure 2, the reason of the present phenomenon was that the stress responses of microbes were stimulated by the toxic substance. It was also an adminicle that the present biofilm had good antitoxicity and stability. From an engineering perspective, it was very useful for fabricating the biosensor in the environmental field that the PI-permeable state could be used for maintaining the catalytic activity of the biosensor under nutrition-poor conditions. The present mechanism was successfully used to explain the long-term stability of biosensors based on many biofilms formed on the other substrates, including graphene-based gel, biomass-based gel, and PVC tubes (Figure 6).

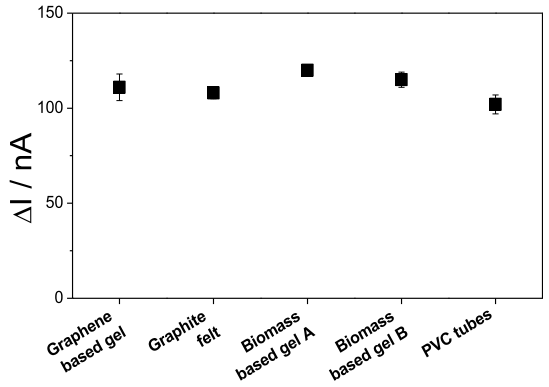

Figure 6. Electrochemical results for measuring GGA20 after two months by using the biosensors based on graphene-based gel, graphite felt, biomass-based gel, and PVC tubes.

The biosensor was integrated into a multiparameter water quality monitoring station on a local lake for BOD detection. As shown in Figure 7, from December 2016 to October 2019, the biosensor was operated stably. Here, three cases were analyzed to illustrate the practical value of the biosensor based on the PI-permeable state of microbes.

(1) As shown in Table S1, the BOD value was increased about 50% between 11 and 15 in November, 2017. Combining with the changes of ammonia nitrogen (NH_3−N) and total nitrogen (TN), the pollution of water was confirmed. Similar cases happened between October and December 2017 and between January and March 2019.

(2) In September 2017, DO values were below 2 mg L^{-1} and the values of BOD, NH_3−N, and TN were higher than that for the ordinary measurements in a certain time. This result indicated that the microbial activity in the water was enhanced by those organic pollutions, leading to a mount of fermentation and the DO was reduced. According to the present research, a condition of poor nutrition and low temperature should be adjusted for the present biosensor. After a period of control, the state of the biosensor was recovered (Table S2).

(3) The values of BOD were higher than those by the ordinary measuring and the DO were below 3 mg L^{-1}, but the values of NH_3−N and TN did not change significantly. It could be judged that a simple overgrowth of the biofilm in the biosensor happened, and the nutrition condition should be controlled for the recovery of sensor's values. Thus, the effective measurements and the biofeedback of water pollution could be accurately reflected based on the guiding by the present theory (Table S3).

CONCLUSIONS

In this work, we fabricated a biosensor based on the PI-permeable state microbes. This biosensor showed excellent stability. What is more, this work demonstrated that except dead or live states, there was an intermediate state. In this state, the catalytic activity still existed, which resulted in long-term

https://dx.doi.org/10.1021/acssensors.9b02138
ACS Sens. 2020, 5, 258−264

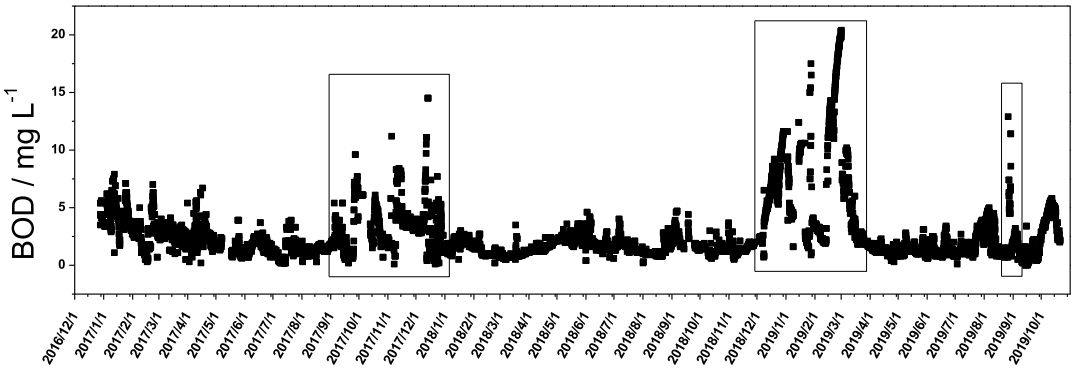

Figure 7. Record of the BOD for monitoring water pollution of a local lake from Dec 2016 to Oct 2019.

stability of the biosensor and made the practical application of the biosensor possible.

■ ASSOCIATED CONTENT

Supporting Information

The Supporting Information is available free of charge at https://pubs.acs.org/doi/10.1021/acssensors.9b02138.

Scheme of biofilm assay and suspended assay; CLSM images of the suspended microbes treated with the heavy metal ion; CLSM images for characterizing the PI-stained ratio in the process of biofilm formation; optical photos of biofilm; CLSM images of the new cultured nutrient enrichment biofilm and after it was used for GGA measurements; 16s DNA analysis: species profiling the histogram at the phylum level; calibration curve and measurements of the real sample by using the biosensor based on the PI-permeable biofilm; long-term stability of the present biosensor; *I*−*t* curves for measuring the organic substance GGA and toxic substance; and data recorded by the multiparameter water quality monitoring station on a local lake (PDF)

■ AUTHOR INFORMATION

Corresponding Authors

Ling Liu − *Chinese Academy of Sciences, Changchun, PR China*; Email: liuling@ciac.ac.cn

Shaojun Dong − *Chinese Academy of Sciences, Changchun, PR China*; orcid.org/0000-0002-0263-6577; Email: dongsj@ciac.ac.cn

Other Authors

Changyu Liu − *Chinese Academy of Sciences, Changchun, PR China, and Wuyi University, Jiangmen, PR China*

He Zhang − *Chinese Academy of Sciences, Changchun, PR China*

Jingting He − *Chinese Academy of Sciences, Changchun, PR China, and Jinzhou Medical University, Jinzhou, PR China*

Junfeng Zhai − *Chinese Academy of Sciences, Changchun, PR China*; orcid.org/0000-0001-5421-6999

Dengbin Yu − *Chinese Academy of Sciences, Changchun, PR China*

Complete contact information is available at: https://pubs.acs.org/10.1021/acssensors.9b02138

Notes

The authors declare no competing financial interest.

■ ACKNOWLEDGMENTS

This work was supported by the National Natural Science Foundation of China (grant no. 21675151), MOST, China (grant no. 2016YFA0203203).

■ REFERENCES

(1) Ferrer, M. L.; Yuste, L.; Rojo, F.; del Monte, F. Biocompatible sol-gel route for encapsulation of living bacteria in organically modified silica matrixes. *Chem. Mater.* **2003**, *15*, 3614−3618.

(2) Wong, L. S.; Lee, Y. H.; Surif, S. Whole cell biosensor using anabaena torulosa with optical transduction for environmental toxicity evaluation. *J. Sens.* **2013**, *2013*, 1.

(3) Rijavec, T.; Zrimec, J.; Oven, F.; Viršek, M. K.; Somrak, M.; Podlesek, Z.; Gostinčar, C.; Leedjärv, A.; Virta, M.; Tratnik, J. S.; Horvat, M.; Lapanje, A. Development of highly sensitive, Automatized and portable whole-cell Hg biosensor based on environmentally relevant microorganisms. *Geomicrobiol. J.* **2017**, *34*, 596−605.

(4) Chee, G.-J. A novel whole-cell biosensor for the determination of trichloroethylene. *Sens. Actuators, B* **2016**, *237*, 836−840.

(5) Perullini, M.; Jobbágy, M.; Bermúdez Moretti, M.; Correa García, S.; Bilmes, S. A. Optimizing silica encapsulation of living cells: In situ evaluation of cellular stress. *Chem. Mater.* **2008**, *20*, 3015−3021.

(6) Cui, Z.; Luan, X.; Jiang, H.; Li, Q.; Xu, G.; Sun, C.; Zheng, L.; Song, Y.; Davison, P. A.; Huang, W. E. Application of a bacterial whole cell biosensor for the rapid detection of cytotoxicity in heavy metal contaminated seawater. *Chemosphere* **2018**, *200*, 322−329.

(7) Castellón, E.; Chavarría, M.; de Lorenzo, V.; Zayat, M.; Levy, D. An electro-optical device from a biofilm structure created by bacterial activity. *Adv. Mater.* **2010**, *22*, 4846−4850.

(8) Cheng, K. Y.; Ho, G.; Cord-Ruwisch, R. Affinity of microbial fuel cell biofilm for the anodic potential. *Environ. Sci. Technol.* **2008**, *42*, 3828−3834.

(9) Schulte, L. N.; Heinrich, B.; Janga, H.; Schmeck, B. T.; Vázquez, O. A far-red fluorescent DNA binder for interaction studies of live multidrug-resistant pathogens and host cells. *Angew. Chem., Int. Ed.* **2018**, *57*, 11564−11568.

(10) Ronen, A.; Semiat, R.; Dosoretz, C. G. Impact of ZnO embedded feed spacer on biofilm development in membrane systems. *Water Res.* **2013**, *47*, 6628−6638.

(11) Ranmadugala, D.; Ebrahiminezhad, A.; Manley-Harris, M.; Ghasemi, Y.; Berenjian, A. The effect of iron oxide nanoparticles on Bacillus subtilis biofilm, growth and viability. *Process Biochem.* **2017**, *62*, 231−240.

(12) Xu, Y.; Wang, X.; Zhang, W. L.; Lv, F.; Guo, S. Recent progress in two-dimensional inorganic quantum dots. *Chem. Soc. Rev.* **2018**, *47*, 586−625.

(13) Chua, S. L.; Yam, J. K. H.; Hao, P.; Adav, S. S.; Salido, M. M.; Liu, Y.; Givskov, M.; Sze, S. K.; Tolker-Nielsen, T.; Yang, L. Selective labelling and eradication of antibiotic-tolerant bacterial populations in Pseudomonas aeruginosa biofilms. *Nat. Commun.* **2016**, *7*, 10750.
(14) Liu, S.; Gunawan, C.; Barraud, N.; Rice, S. A.; Harry, E. J.; Amal, R. Understanding, monitoring, and controlling biofilm growth in drinking water distribution systems. *Environ. Sci. Technol.* **2016**, *50*, 8954−8976.
(15) Chung, C. Y.-S.; Fung, S.-K.; Tong, K.-C.; Wan, P.-K.; Lok, C.-N.; Huang, Y.; Chen, T.; Che, C.-M. A multi-functional PEGylated gold(III) compound: potent anti-cancer properties and self-assembly into nanostructures for drug co-delivery. *Chem. Sci.* **2017**, *8*, 1942−1953.
(16) Liu, C.; Faria, A. F.; Ma, J.; Elimelech, M. Mitigation of biofilm development on thin-film composite membranes functionalized with zwitterionic polymers and silver nanoparticles. *Environ. Sci. Technol.* **2017**, *51*, 182−191.
(17) Lee, W. H.; Pressman, J. G.; Wahman, D. G. Three-dimensional free chlorine and monochloramine biofilm penetration: correlating penetration with biofilm activity and viability. *Environ. Sci. Technol.* **2018**, *52*, 1889−1898.
(18) Caruso, G.; Mancuso, M.; Crisafi, E. Combined fluorescent antibody assay and viability staining for the assessment of the physiological states of Escherichia coli in seawaters. *J. Appl. Microbiol.* **2003**, *95*, 225−233.
(19) Kepp, O.; Galluzzi, L.; Lipinski, M.; Yuan, J.; Kroemer, G. Cell death assays for drug discovery. *Nat. Rev. Drug Discovery* **2011**, *10*, 221−237.
(20) Czechowska, K.; Johnson, D. R.; van der Meer, J. R. Use of flow cytometric methods for single-cell analysis in environmental microbiology. *Curr. Opin. Microbiol.* **2008**, *11*, 205−212.
(21) Nebe-von-Caron, G.; Stephens, P. J.; Hewitt, C. J.; Powell, J. R.; Badley, R. A. Analysis of bacterial function by multi-colour fluorescence flow cytometry and single cell sorting. *J. Microbiol. Methods* **2000**, *42*, 97−114.
(22) Yang, Y.; Xiang, Y.; Xu, M. From red to green: the propidium iodide-permeable membrane of Shewanella decolorationis S12 is repairable. *Sci. Rep.* **2016**, *5*, 18583.
(23) Zhu, Y.; Clair, G.; Chrisler, W. B.; Shen, Y.; Zhao, R.; Shukla, A. K.; Moore, R. J.; Misra, R. S.; Pryhuber, G. S.; Smith, R. D.; Ansong, C.; Kelly, R. T. Proteomic analysis of single mammalian cells enabled by microfluidic nanodroplet sample preparation and ultrasensitive nanoLC-MS. *Angew. Chem., Int. Ed.* **2018**, *57*, 12370−12374.
(24) Azuma, Y.; Imai, H.; Kawaguchi, Y.; Nakase, I.; Kimura, H.; Futaki, S. Modular redesign of a cationic lytic peptide to promote the endosomal escape of biomacromolecules. *Angew. Chem., Int. Ed.* **2018**, *57*, 12771−12774.
(25) de Castro, A. G.; Lapinski, J.; Tunnacliffe, A. Anhydrobiotic engineering. *Nat. Biotechnol.* **2000**, *18*, 473.
(26) Song, J.; Xu, C.-H.; Huang, S.-Z.; Lei, W.; Ruan, Y.-F.; Lu, H.-J.; Zhao, W.; Xu, J.-J.; Chen, H.-Y. Ultrasmall nanopipette: toward continuous monitoring of redox metabolism at subcellular level. *Angew. Chem., Int. Ed.* **2018**, *57*, 13226−13230.
(27) Zhang, X.; Zhuchenko, O.; Kuspa, A.; Soldati, T. Social amoebae trap and kill bacteria by casting DNA nets. *Nat. Commun.* **2016**, *7*, 10938.
(28) Rice, K. C.; Mann, E. E.; Endres, J. L.; Weiss, E. C.; Cassat, J. E.; Smeltzer, M. S.; Bayles, K. W. The cidA murein hydrolase regulator contributes to DNA release and biofilm development in Staphylococcus aureus. *Proc. Natl. Acad. Sci. U.S.A.* **2007**, *104*, 8113−8118.
(29) Liu, L.; Zhai, J.; Zhu, C.; Gao, Y.; Wang, Y.; Han, Y.; Dong, S. One-pot synthesis of 3-dimensional reduced graphene oxide-based hydrogel as support for microbe immobilization and BOD biosensor preparation. *Biosens. Bioelectron.* **2015**, *63*, 483−489.
(30) Yu, D.; Zhai, J.; Yong, D.; Dong, S. A rapid and sensitive p-benzoquinone-mediated bioassay for determination of heavy metal toxicity in water. *Analyst* **2013**, *138*, 3297−3302.
(31) Zhou, L.; Li, T.; An, J.; Liao, C.; Li, N.; Wang, X. Subminimal inhibitory concentration (sub-MIC) of antibiotic induces electroactive biofilm formation in bioelectrochemical systems. *Water Res.* **2017**, *125*, 280−287.
(32) Ma, L.; Conover, M.; Lu, H.; Parsek, M. R.; Bayles, K.; Wozniak, D. J. Assembly and development of the pseudomonas aeruginosa biofilm matrix. *PLoS Pathog.* **2009**, *5*, No. e1000354.
(33) Xiao, Y.; Zhang, E.; Zhang, J.; Dai, Y.; Yang, Z.; Christensen, H. E. M.; Ulstrup, J.; Zhao, F. Extracellular polymeric substances are transient media for microbial extracellular electron transfer. *Sci. Adv.* **2017**, *3*, No. e1700623.
(34) Xiao, Y.; Zhao, F. Electrochemical roles of extracellular polymeric substances in biofilms. *Curr. Opin. Electrochem.* **2017**, *4*, 206−211.
(35) Rühl, S.; Shkarina, K.; Demarco, B.; Heilig, R.; Santos, J. C.; Broz, P. ESCRT-dependent membrane repair negatively regulates pyroptosis downstream of GSDMD activation. *Science* **2018**, *362*, 956−960.
(36) Jimenez, A. J.; Maiuri, P.; Lafaurie-Janvore, J.; Divoux, S.; Piel, M.; Perez, F. ESCRT machinery is required for plasma membrane repair. *Science* **2014**, *343*, 1247136.

https://dx.doi.org/10.1021/acssensors.9b02138
ACS Sens. 2020, 5, 258−264